Polypropylene Nanocomposites Based on Designed Synthetic Nanoplatelets

Luyi Sun,[†,‡] Jia Liu,[†] Sharath R. Kirumakki,[‡] Eric D. Schwerdtfeger,[‡] Robert J. Howell,[‡] Khalid Al-Bahily,[‡] Stephen A. Miller,[§,‡] Abraham Clearfield,*[,‡] and Hung-Jue Sue*[,†]

Polymer Technology Center, Department of Mechanical Engineering, Texas A&M University, College Station, Texas 77843-3123, and Department of Chemistry, Texas A&M University, College Station, Texas 77842-3012

Received November 6, 2008. Revised Manuscript Received January 26, 2009

Synthetic nanoplatelets derived from α-zirconium phosphate (α-ZrP) were prepared for in situ propylene polymerization, yielding polypropylene (PP) nanocomposites. The designed α-ZrP-derivatives contain methyl groups on the surface to increase hydrophobicity, which gives rise to a better compatibility with toluene and propylene molecules. The incorporation of methyl groups on the layers of α-ZrP-derivatives also produces a "porous pathway" structure in the nanoplatelet gallery, which facilitates the diffusion of propylene monomers. PP/α-ZrP nanocomposites were successfully prepared with a high level of exfoliation. The implications of the present findings are discussed.

Introduction

Since the successful preparation of nylon/clay nanocomposites by Toyota researchers more than two decades ago,[1−4] significant research and development activities have been carried out to prepare other high-performance polymer nanocomposites.[5−7] Although some accomplishments have been reported on the preparation of polar-polymer-based nanocomposites, there has not been much success in the preparation of nonpolar-polymer-based nanocomposites. In particular, preparation of polypropylene (PP) nanocomposites appears to be most challenging. The low compatibility between PP and inorganic nanoplatelets leads to poor dispersion and adhesion of nanoplatelets in the PP matrix, resulting in low performance of PP nanocomposites. However, because of the significant commercial importance and wide applications of PP, it has been highly desirable to prepare PP nanocomposites with high performance. If PP nanocomposites can exhibit a similar level of mechanical and thermal property improvement as in the case of nylon/clay nanocomposites, it would dramatically enhance the competitiveness of PP for various engineering applications.

In general, the morphology of nanoplatelets dispersion is determined by the interplay of entropic and enthalpic factors.[8−11] Dispersion of regular hydrophilic nanofillers in a polymer matrix requires sufficiently favorable enthalpic contributions to overcome any entropic penalties.[11] The most typical approaches to overcome the above requirements are either PP functionalization or organic modification of the nanofillers, or both. The most common PP functionalization is via grafting of maleic anhydride functionality to PP chains (PP-*g*-Ma). By mixing PP-*g*-Ma together with organically modified nanoplatelets, which typically follows a compounding procedure to prepare a masterbatch and a subsequent blending with pristine PP, good improvements in mechanical properties have been achieved.[12−22] Other attempts using hydroxyl-,[23−25] amine-,[12,23,25,26] and halogen-functionalized[25] PP for better inorganic nanoplatelet dispersion have also been

* To whom correspondence should be addressed. Tel: (979) 845-5024 (H.-J.S.); (979) 845-2936 (A.C.). Fax: (979) 845-3081 (H.-J.S.); (979) 845-2370 (A.C.). E-mail: hjsue@tamu.edu (H.-J.S.); clearfield@mail.chem.tamu.edu (A.C.).
† Department of Mechanical Engineering, Texas A&M University.
‡ Department of Chemistry, Texas A&M University.
§ Present address: Department of Chemistry, University of Florida, Gainesville, Florida 32611.

(1) Okada, A.; Usuki, A. *Macromol. Mater. Eng.* **2006**, *291*, 1449–1476.
(2) Usuki, A.; Kojima, Y.; Kawasumi, M.; Okada, A.; Fukushima, Y.; Kurauchi, T.; Kamigaito, O. *J. Mater. Res.* **1993**, *8*, 1179–1184.
(3) Kojima, Y.; Usuki, A.; Kawasumi, M.; Okada, A.; Fukushima, Y.; Kurauchi, T.; Kamigaito, O. *J. Mater. Res.* **1993**, *8*, 1185–1189.
(4) Kojima, Y.; Usuki, A.; Kawasumi, M.; Okada, A.; Kurauchi, T.; Kamigaito, O. *J. Polym. Sci., Part A: Polym. Chem.* **1993**, *31*, 983–986.
(5) Giannelis, E. P. *Adv. Mater.* **1996**, *8*, 29–35.
(6) Alexandre, M.; Dubois, P. *Mater. Sci. Eng., R* **2000**, *28*, 1–63.
(7) Ray, S. S.; Okamoto, M. *Prog. Polym. Sci.* **2003**, *28*, 1539–1641.
(8) Vaia, R. A.; Giannelis, E. P. *Macromolecules* **1997**, *30*, 7990–7999.
(9) Vaia, R. A.; Giannelis, E. P. *Macromolecules* **1997**, *30*, 8000–8009.
(10) Balazs, A. C.; Singh, C.; Zhulina, E. *Macromolecules* **1998**, *31*, 8370–8381.
(11) Manias, E.; Touny, A.; Wu, L.; Strawhecker, K.; Lu, B.; Chung, T. C. *Chem. Mater.* **2001**, *13*, 3516–3523.
(12) Kato, M.; Usuki, A.; Okada, A. *J. Appl. Polym. Sci.* **1997**, *66*, 1781–1785.
(13) Kawasumi, M.; Hasegawa, N.; Kato, M.; Usuki, A.; Okada, A. *Macromolecules* **1997**, *30*, 6333–6338.
(14) Hasegawa, N.; Kawasumi, M.; Kato, M.; Usuki, A.; Okada, A. *J. Appl. Polym. Sci.* **1998**, *67*, 87–92.
(15) Hasegawa, N.; Okamoto, H.; Kawasumi, M.; Kato, M.; Tsukigase, A.; Usuki, A. *Macromol. Mater. Eng.* **2000**, *280*, 76–79.
(16) Nam, P. H.; Maiti, P.; Okamoto, M.; Kotaka, T.; Hasegawa, N.; Usuki, A. *Polymer* **2001**, *42*, 9633–9640.
(17) Marchant, D.; Jayaraman, K. *Ind. Eng. Chem. Res.* **2002**, *41*, 6402–6408.
(18) Hasegawa, N.; Usuki, A. *J. Appl. Polym. Sci.* **2004**, *93*, 464–470.
(19) Kato, M.; Matsushita, M.; Fukumori, K. *Polym. Eng. Sci.* **2004**, *44*, 1205–1211.
(20) Chavarria, F.; Nairn, K.; White, P.; Hill, A. J.; Hunter, D. L.; Paul, D. R. *J. Appl. Polym. Sci.* **2007**, *105*, 2910–2924.
(21) Kim, D. H.; Fasulo, P. D.; Rodgers, W. R.; Paul, D. R. *Polymer* **2007**, *48*, 5308–5323.
(22) Kim, D. H.; Fasulo, P. D.; Rodgers, W. R.; Paul, D. R. *Polymer* **2007**, *48*, 5960–5978.

10.1021/cm803024e CCC: $40.75
Published on Web 03/02/2009

reported. Although the above melt compounding approach does show some success, in situ polymerization is another attractive alternative route for the preparation of PP nanocomposites. If successful, the in situ polymerization approach should be a lower cost alternative and may lead to accelerated commercialization of PP nanocomposites.

Compared to the blending approach, it is experimentally more challenging to prepare PP nanocomposites via in situ polymerization, mainly because of the high sensitivity of the catalysts used for propylene polymerization. Both Ziegler−Natta catalysts and metallocene catalysts are highly sensitive to Lewis bases and water. Surface modifications of nanoplatelets usually involve the usage of amines or quaternary ammonium ions, both of which can easily deactivate catalysts. In addition, the nanoplatelets have to be subjected to pretreatments to remove water before they are incorporated for in situ polymerization. Presently, most of the efforts still focus on the compounding approach to prepare PP nanocomposites; far fewer studies have emphasized the in situ polymerization approach.[27−36] The paucity of literature also highlights the difficulty of using an in situ polymerization approach for PP nanocomposites preparation. Methodology for avoiding the negative effect of the organic modifiers on the catalysts while achieving a high level of dispersion of nanoplatelets in the PP matrix is a key hurdle to overcome.

In most published reports, smectite clays, such as montmorillonite, were used as nanofillers for the preparation of polymer nanocomposites.[5−7] As discussed above, because of their hydrophilic nature, it is thermodynamically unfavorable to disperse them in PP without surface modification. Surface modifications of montmorillonite are limited to noncovalent ion exchange processes, and those surface modifiers will usually poison the catalysts for propylene polymerization. Alternatively, a synthetic layered compound, α-zirconium phosphate ($Zr(HPO_4)_2 \cdot H_2O$, hereafter referred to as α-ZrP), has been systematically studied in the past few years for nanocomposite preparations.[37−47] Because of its synthetic nature, α-ZrP exhibits much higher versatility for the preparation of nanocomposites. Its surface functionality, dimension, and morphology can be manipulated by varying reaction conditions or choosing different synthetic approaches.[48,49] In this paper, we report the preparation of PP/α-ZrP-derivative nanocomposites via an in situ polymerization approach. These novel α-ZrP-derivative nanoplatelets were specifically designed to possess high compatibility with liquid propylene without requiring any surface modification. Meanwhile, the interlayer structure was also designed to form a "porous pathway" to facilitate the insertion of propylene monomers into the gallery.[47] Thus, the designed α-ZrP-derivative nanoplatelets are both thermodynamically and kinetically more favorable for the preparation of PP based nanocomposites than typical natural clays.

Isotactic polypropylene is the commercially important form of the polymer. Polypropylene of very high isotacticity can be prepared using an appropriate Ziegler−Natta catalyst. A variety of C_2-symmetric metallocenes are commercially available for the production of isotactic polypropylene. These catalysts, however, tend to be less isoselective than the best Ziegler−Natta catalysts. Certain C_1-symmetric metallocenes have comparable isoselectivity to the best C_2-symmetric catalysts. Additionally, the C_1-symmetric complexes tend to increase in isoselectivity with increasing polymerization temperature.[50] We have chosen to use a proprietary C_1-symmetric metallocene previously prepared in our laboratory for the preparation of in situ PP nanocomposites. The catalyst used was chosen for its high isoselectivity (at least as good as ethylene(bis indenyl)zirconium dichloride) and convenient synthesis, as well as the rather high molecular weight polymer that is formed.

Experimental Section

Materials. Zirconium oxychloride octahydrate ($ZrOCl_2 \cdot 8H_2O$, 98%, Sigma-Aldrich), phosphoric acid (85%, EM Science), methylphosphonic acid (98%, Sigma-Aldrich), and hydrofluoric acid (48%, EMD Chemicals) were used as received. Toluene was filtered through an MBraun solvent purification system into a Straus flask, degassed under high vacuum to remove residual oxygen, and stored in the Straus flask until needed. A stock solution of precatalyst was made by dissolving 0.189 g of Me_2C[(1-Me-4-*t*-Bucyclohexyl)C_5H_3][$C_{13}H_8$]$ZrCl_2$ (**1**) in toluene in a 100 mL volumetric flask (3.23 mM) in the glovebox. A toluene solution of methylaluminoxane (MAO) was obtained from Albemarle; toluene

(23) Wang, Z. M.; Han, H.; Chung, T. C. *Macromol. Symp.* **2005**, *225*, 113–127.
(24) Usuki, A.; Kato, M.; Okada, A.; Kurauchi, T. *J. Appl. Polym. Sci.* **1997**, *63*, 137–139.
(25) Chung, T. C. *J. Organomet. Chem.* **2005**, *690*, 6292–6299.
(26) Cui, L.; Paul, D. R. *Polymer* **2007**, *48*, 1632–1640.
(27) Tudor, J.; Willington, L.; O'Hare, D.; Royan, B. *Chem. Commun.* **1996**, 2031–2032.
(28) Bergman, J. S.; Chen, H.; Giannelis, E. P.; Thomas, M. G.; Coates, G. W. *Chem. Commun.* **1999**, 2179–2180.
(29) Sun, T.; Garces, J. M. *Adv. Mater.* **2002**, *14*, 128–130.
(30) He, A.; Hu, H.; Huang, Y.; Dong, J.-Y.; Han, C. C. *Macromol. Rapid Commun.* **2004**, *25*, 2008–2013.
(31) Hwu, J.-M.; Jiang, G.-J. *J. Appl. Polym. Sci.* **2005**, *95*, 1228–1236.
(32) Reddy, C. S.; Das, C. K. *J. Macromol. Sci., Part A: Pure Appl. Chem.* **2006**, *43*, 1365–1378.
(33) He, A.; Wang, L.; Li, J.; Dong, J.; Han, C. C. *Polymer* **2006**, *47*, 1767–1771.
(34) Reddy, C. S.; Kumar Das, C. *J. Polym. Res.* **2007**, *14*, 129–139.
(35) Du, K.; He, A. H.; Liu, X.; Han, C. C. *Macromol. Rapid Commun.* **2007**, *28*, 2294–2299.
(36) Yang, K.; Huang, Y.; Dong, J.-Y. *Polymer* **2007**, *48*, 6254–6261.
(37) Sue, H.-J.; Gam, K. T.; Bestaoui, N.; Spurr, N.; Clearfield, A. *Chem. Mater.* **2004**, *16*, 242–249.
(38) Sue, H.-J.; Gam, K. T.; Bestaoui, N.; Clearfield, A.; Miyamoto, M.; Miyatake, N. *Acta Mater.* **2004**, *52*, 2239–2250.
(39) Sun, L.; Boo, W. J.; Browning, R. L.; Sue, H.-J.; Clearfield, A. *Chem. Mater.* **2005**, *17*, 5606–5609.
(40) Sun, L.; Boo, W. J.; Sue, H.-J.; Clearfield, A. *New J. Chem.* **2007**, *31*, 39–43.
(41) Sun, L.; Boo, W. J.; Sun, D.; Clearfield, A.; Sue, H.-J. *Chem. Mater.* **2007**, *19*, 1749–1754.
(42) Sun, L.; Boo, W. J.; Clearfield, A.; Sue, H.-J.; Pham, H. Q. *J. Membr. Sci.* **2008**, *318*, 129–136.
(43) Sun, L.; Boo; W.-J.; Liu, J.; Clearfield, A.; Sue, H.-J.; Verghese, N. E.; Pham, H. Q.; Bicerano, J. *Macromol. Mater. Eng.* **2009**, *294*, 103–113.
(44) Boo, W. J.; Sun, L.; Liu, J.; Clearfield, A.; Sue, H.-J.; Mullins, M. J.; Pham, H. *Compos. Sci. Technol.* **2007**, *67*, 262–269.
(45) Boo, W. J.; Sun, L.; Liu, J.; Moghbelli, E.; Clearfield, A.; Sue, H.-J.; Pham, H.; Verghese, N. *J. Polym. Sci., Part B: Polym. Phys.* **2007**, 1459–1469.
(46) Boo, W. J.; Sun, L.; Warren, G. L.; Moghbelli, E.; Pham, H.; Clearfield, A.; Sue, H.-J. *Polymer* **2007**, *48*, 1075–1082.
(47) Boo, W. J.; Sun, L.; Liu, J.; Clearfield, A.; Sue, H.-J. *J. Phys. Chem. C* **2007**, *111*, 10377–10381.
(48) Alberti, G. *Acc. Chem. Res.* **1978**, *11*, 163–170.
(49) Clearfield, A. *Annu. Rev. Mater. Sci.* **1984**, *14*, 205–229.
(50) Miller, S. A.; Bercaw, J. E. *Organometallics* **2006**, *25*, 3576–3592.

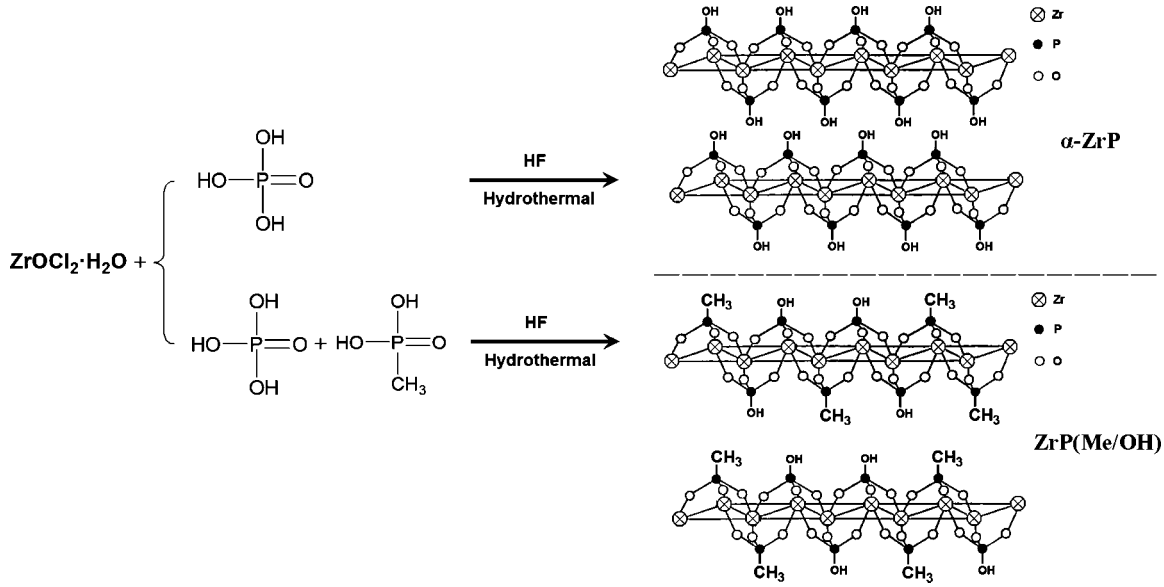

Figure 1. Schematic of the reaction for the synthesis of α-ZrP and its methyl/hydroxyl mixed derivative.

Table 1. Formulation and Reaction Conditions for the Synthesis of α-ZrP and Its Methyl/Hydroxyl Mixed Derivatives

	formulation			reaction conditions		
sample	molar ratio of $CH_3P(O)(OH)_2$:H_3PO_4	atomic ratio of Zr:P	HF (Zr:F)	medium	temperature (°C)	time (days)
α-ZrP	H_3PO_4 only	1:20	No HF	H_2O	200	1
$ZrP(Me_1/OH_2)$	1:2	1:2	1:4	H_2O	105	4
$ZrP(Me_1/OH_1)$	1:1	1:2	1:3	H_2O	105	4
$ZrP(Me_2/OH_1)$	2:1	1:2	1:4	H_2O	105	4

was removed under a vacuum, and the solid was dried at 70 °C for 3 days to remove any residual $AlMe_3$. Both the stock solution and MAO powder were stored in the glovebox.

Synthesis of α-ZrP and Its Derivatives. The α-ZrP methyl/hydroxyl mixed derivatives [ZrP(Me/OH)] were synthesized via a hydrothermal method with $ZrOCl_2 \cdot 8H_2O$, methylphosphonic acid [$CH_3P(O)(OH)_2$], and phosphoric acid (H_3PO_4) as starting materials in the presence of a complexing agent, HF.[51,52] Three ZrP(Me/OH) mixed derivatives were prepared by adjusting the ratio between methylphosphonic acid and phosphoric acid. During the reaction, both methylphosphonic acid and phosphoric acid molecules were randomly incorporated into the layers, forming a layered structure with methyl and hydroxyl groups pointing to the interlayer space. The detailed chemistry regarding the synthesis of α-ZrP derivatives can be found elsewhere[52−55] and is schematically illustrated in Figure 1. α-ZrP was also synthesized via a similar hydrothermal approach and used as a control.[40,49] The formulations and reaction conditions for the synthesis of the above α-ZrP derivatives are summarized in Table 1. The detailed preparation procedures are provided in the Supporting Information.

Synthesis of Precatalyst $Me_2C[(4\text{-t-Bu-1-Me-cyclohexyl})C_5H_3][C_{13}H_8]ZrCl_2$ (1).[56] *1-t-Butyl-4-cyclopenta-2,4-dienylidene-cyclohexane.* A 500 mL round-bottom flask was charged with 50 mL (605 mmol) of cyclopentadiene, 46.5 g (302 mmol) of 4-*t*-butylcyclohexanone, and 250 mL of methanol. Then 5.0 mL (60 mmol) of pyrrolidine were syringed in. After being stirred for 21 h, the yellow precipitate was filtered and refluxed in 200 mL of methanol for 1 h. After being cooled, the product was filtered and dried in a vacuum line to give 37.51 g (61.51%) of product. MS (EI) *m*/*z* 202 (M^+).

Table 2. Composition of Synthesized PP/ZrP(Me/OH) Nanocomposites

sample	treatment on ZrP(Me/OH)	ZrP(Me/OH) loading (wt %)	melting temperature (°C)
1 PP			147.1
2 $PP/ZrP(Me_1/OH_2)$	ultrasonication	1.3	143.8
3 $PP/ZrP(Me_1/OH_1)$	ultrasonication	0.4	149.7
4 $PP/ZrP(Me_1/OH_1)$	no	1.2	147.9

(4-t-Butyl-1-methylcyclohexyl)cyclopentadiene. A 500 mL round-bottom flask was charged with 9.1 g (45 mmol) of 1-*t*-butyl-4-cyclopenta-2,4-dienylidene-cyclohexane. The flask then was equipped with a 180° needle valve and evacuated. Then 60 mL of diethyl ether were syringed in, and at 0 °C, 60 mL (135 mmol) of methyllithium (1.5 M in diethyl ether) were syringed in followed by 6 mL of dimethoxyethane. After being stirred for 48 h, 60 mL of NH_4Cl solution were added at 0 °C. The organic layer was isolated and the aqueous layer was extracted with diethyl ether (3 × 25 mL). The combined organic layers were dried over $MgSO_4$ and filtered. The solution was rotovapped to give 9.30 g (99.8%) of product as a yellow oil. MS (EI) *m*/*z* 218 (M^+).

3-(4-t-Butyl-1-methylcyclohexyl)-6,6-dimethylfulvene. In a 500 mL flask, (4-*t*-butyl-1-methylcyclohexyl)cyclopentadiene (10.05 g, 46.06 mmol), 18.0 mL (245 mmol) of acetone, and 80 mL of methanol were mixed together. After a homogeneous solution was obtained, 6.0 mL (72 mmol) of pyrrolidine were added slowly. After

(51) Alberti, G.; Torracca, E. *J. Inorg. Nucl. Chem.* **1968**, *30*, 317–318.
(52) Alberti, G.; Costantino, U.; Allulli, S.; Tomassini, N. *J. Inorg. Nucl. Chem.* **1978**, *40*, 1113–1117.
(53) Wang, J. D.; Clearfield, A.; Peng, G.-Z. *Mater. Chem. Phys.* **1993**, *35*, 208–216.
(54) Cabeza, A.; Ouyang, X.; Sharma, C. V. K.; Aranda, M. A. G.; Bruque, S.; Clearfield, A. *Inorg. Chem.* **2002**, *41*, 2325–2333.
(55) Segawa, K.; Funamoto, T.; Ando, J.; Yamaguchi, C.; Kaneko, K.; Takeoka, Y.; Rikukawa, M.; Steen, E. v.; Claeys, I. M.; Callanan, L. H. In *Studies in Surface Science and Catalysis*; Elsevier: Amsterdam, The Netherlands, 2004; Vol. 154, Part 1, pp 1096−1102.
(56) Al-Bahily, K. A. Masters Thesis, Texas A&M University, College Station, TX, 2004.

Table 3. Preparation of Synthesized PP/ZrP(Me/OH) Nanocomposites

sample	filler (g)	toluene (mL)	propylene (mL)	catalyst (μmol)	MAO equiv	time (min)	yield (g)	[*mmmm*]	activity (kg/(mol h))
1	0	20	20	3.89	2500	2	4.22	0.941	32500
2	0.1	0	40	7.77	5000	10	7.63	0.91	5890
3	0.3	100	400	6.46	5000	60	73.34		11400
4	0.3	100	400	6.46	5000	30	21.32		6600

the solution was stirred for 72 h, 7 mL of acetic acid and 300 mL of water were added followed by 100 mL of diethyl ether. The organic layer was isolated and the aqueous layer was extracted with diethyl ether (4 × 50 mL). The combined organic layers were extracted with H_2O (3 × 50 mL) and then 10% sodium hydroxide solution (3 × 30 mL). The combined organic layers were dried over $MgSO_4$, filtered, and rotovapped to give 11.21 g (94.28%) of product as an orange oil. MS (EI) *m*/*z* 258 (M^+).

Me_2C[3-(4-t-Bu-1-Me-cyclohexyl)C_5H_3][$C_{13}H_8$]H_2. In the glovebox, a 500 mL round-bottom flask was charged with 7.74 g (30.0 mmol) of 3-(4-*t*-butyl-1-methylcyclohexyl)-6,6-dimethylfulvene and 80 mL of diethyl ether. Then 5.16 g (30.0 mmol) of fluorenyllithium were added to the solution. After the solution was stirred for 96 h under a nitrogen atmosphere, 60 mL of of NH_4Cl solution was added. The organic layer was isolated and the aqueous layer was extracted with diethyl ether (3 × 50 mL). The combined organic layers were dried over $MgSO_4$, filtered, and rotovapped to give 11.64 g (91.50%) of product as an orange oil. MS (MALDI) *m*/*z* 425 $(M+H)^+$.

*Me_2C[3-(4-t-Bu-1-Me-cyclohexyl)C_5H_3][$C_{13}H_8$]$ZrCl_2$ (**1**).* In the glovebox, a 100 mL round-bottom flask was charged with 11.26 g (26.53 mmol) of Me_2C[3-(4-*t*-Bu-1-Me-cyclohexyl)C_5H_3][$C_{13}H_8$]-H_2 and 60 mL of diethyl ether. The flask then was attached to a swivel frit. At 0 °C, 23.1 mL of *n*-BuLi (53.06 mmol, 2.3 M in hexanes) were syringed in and stirred for 48 h at room temperature. The solid was removed by filtration (0.81 g of impurity). The solvent was then removed by vacuum and 5.77 g (24.7 mmol) of $ZrCl_4$ was added; 80 mL of diethyl ether were then condensed in. The reaction was stirred for 48 h, followed by solvent removal by a vacuum. Then 70 mL of methylene chloride were condensed in, stirred, and filtered by flipping the swivel frit; the solvent was then removed by vacuum. After that, 60 mL of diethyl ether was condensed in and stirred. The product was isolated by filtration and dried by high vacuum to give 4.65 g (30%) of product as a pink powder. ^{1}H NMR ($CDCl_3$, 300 MHz) δ 0.84 (s, 9H, *t*-butyl-*H*), 1.25 (s, 3H, Me-*H*), 0.80−2.19 (m, 9H, cyclohexyl-*H*), 2.36, 2.39 (s, 6H, $(CH_3)_2$C-Flu-Cp), 5.72, 5.84, 6.19 (t, $^3J_{HH}$ = 2.7, 3.3, 2.3 Hz, 3H, Cp-*H*), 7.23, 7.29, 8.12, 8.15 (d, $^3J_{HH}$ = 6.0, 5.9, 6.9, 6.1 Hz, 4H, Flu-*H*), 7.54, 7.54, 7.82, 7.82 (t, $^3J_{HH}$ = 8.1, 8.1, 8.7, 8.7 Hz, 4H, Flu-*H*). The crystal structure of Me_2C[3-(4-*t*-Bu-1-Me-cyclohexyl)C_5H_3][$C_{13}H_8$]$ZrCl_2$ (**1**) is shown in the Supporting Information.

Preparation of PP/ZrP(Me/OH) Nanocomposites. ZrP(Me/OH) mixed derivatives were treated via two different approaches to prepare nanocomposites. In the first method, ZrP(Me/OH) mixed derivatives were ultrasonicated in toluene for 6 h in an ultrasonication bath (1510R, Branson; 70 W, 42 kHz). It was reasoned that this treatment would facilitate introduction of toluene between the layers due to weakened layer−layer attraction of the mixed derivative and the greater hydrophobic character of the layers. Furthermore, the greater porosity between the layers resulting from the difference in size of the two pendant groups should facilitate the solvation and potential exfoliation of ZrP(Me/OH) in toluene before in situ polymerization. In the second method, no pretreatment was performed on the ZrP(Me/OH) mixed derivatives. After being mixed in toluene, it was directly used for in situ polymerization. During the process, most operations were carried out in a glovebox to avoid moisture and oxygen contamination.

For the preparation of PP/ZrP(Me/OH) nanocomposites, solid MAO and ZrP(Me/OH) (in toluene) were added to a reactor in a glovebox. A stock solution of precatalyst was drawn into a 5 mL Hamilton gastight syringe equipped with a 12 in. needle that was capped with a septum. The reactor was sealed and removed from the box, where it was pressurized with propylene and cooled to 0 °C. The propylene feed continued until the appropriate amount of propylene had been condensed into the reactor, which was then sealed and allowed to stir at 0 °C for 30 min. After this time, the precatalyst solution was injected into the reactor. The reaction was continued for 10 min and stopped through a combination of venting the reactor and injecting a solution of 10% concentrated aqueous HCl in methanol. More acidic methanol (∼400 mL) was used to wash the polymer from the reactor into a 600 mL beaker where it was stirred overnight before being collected by filtration, thrice washed with fresh methanol, and dried under a vacuum to give the final product. The prepared nanocomposites and their compositions are listed in Table 2; the specific synthetic conditions are detailed in Table 3. A neat isotactic PP sample was prepared via the same procedure and used as a control.

Characterizations. X-ray powder diffraction (XRD) patterns were recorded using a Bruker D8 diffractometer with Bragg−Brentano $\theta-2\theta$ geometry (40 kV and 40 mA), using a graphite monochromator with Cu Kα radiation. The nanofiller powder samples and PP nanocomposite fluff samples were gently packed in a sample holder for XRD characterization. The ultrasonicated α-ZrP and ZrP(Me/OH) mixed derivatives were cast as a thin film on a clean silicon wafer and dried overnight at room temperature prior to XRD characterization.

Scanning electron microscopy (SEM) images were acquired on a Zeiss Leo 1530 VP field emission-SEM (FE-SEM). The samples were sputter coated with a thin layer (ca. 3 nm) of Pt/Pd (80/20) prior to the SEM imaging.

Transmission electron microscopy (TEM) images of nanocomposites were obtained using a JEOL 1200 EX transmission electron microscope operated at 100 kV. A Reichert-Jung Ultracut-E microtome was utilized to prepare thin sections of nanocomposites with thickness of 70−100 nm. The thin sections were deposited on carbon coated Cu grids for TEM imaging.

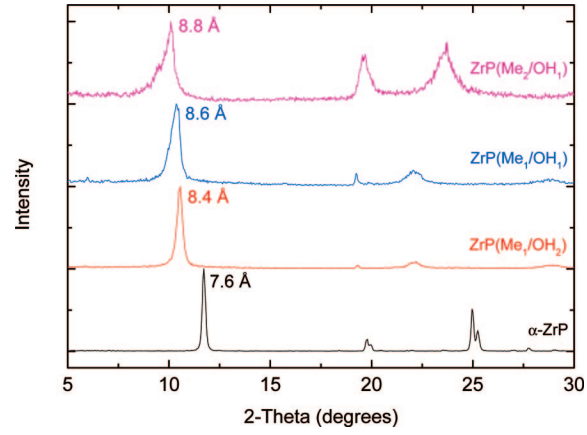

Figure 2. XRD patterns of α-ZrP and its methyl/hydroxyl mixed derivatives.

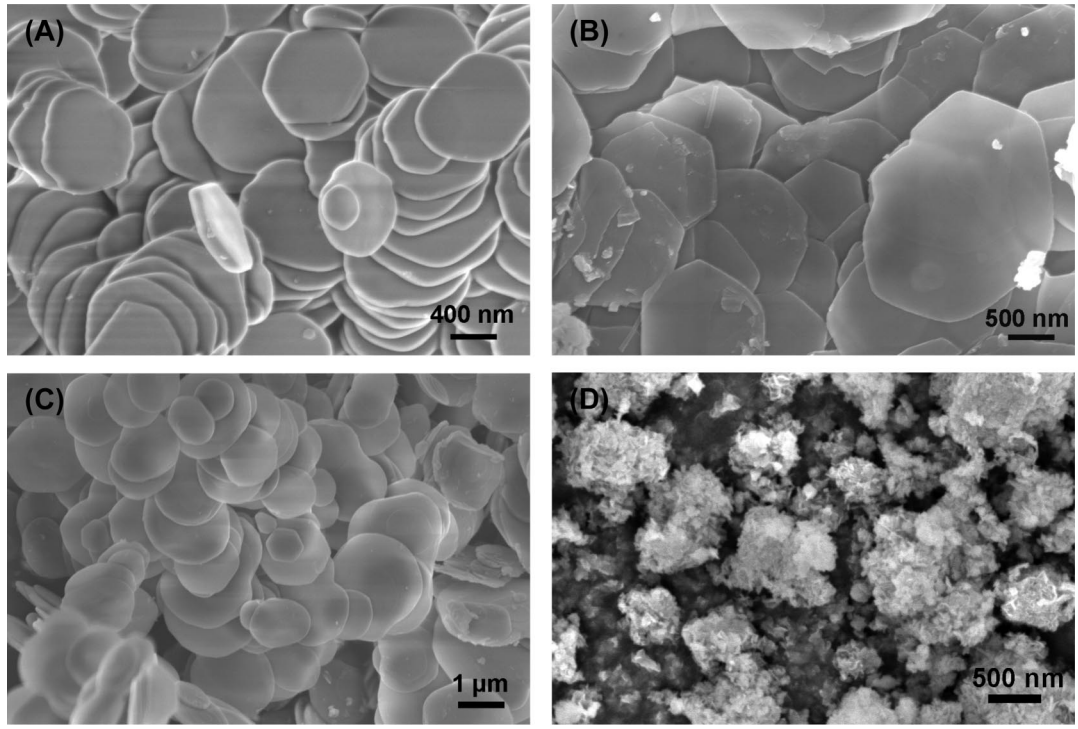

Figure 3. SEM image of (A) α-ZrP and its methyl/hydroxyl mixed derivatives: (B) $ZrP(Me_1/OH_2)$; (C) $ZrP(Me_1/OH_1)$; and (D) $ZrP(Me_2/OH_1)$.

A Mettler Toledo (model DSC821e) differential scanning calorimeter (DSC) was used to obtain the melting temperature of the prepared nanocomposites. The melting temperature data were recorded at the second heating cycle at a heating rate of 10 °C/min under a nitrogen gas purge.

Results and Discussion

Synthesis of ZrP(Me/OH) Mixed Derivatives. The aim of this work is to design and synthesize nanoplatelets that are thermodynamically compatible with hydrophobic nonpolar monomers/polymers and kinetically feasible to be intercalated/exfoliated by these monomers/polymers at a reasonable rate. In this way, these nanoplatelets can be potentially used directly (or after very brief treatment) for the preparation of PP (or other nonpolar polymers) nanocomposites. Introducing methyl groups into the interlayers serves three main functions: (1) introduce methyl groups onto the surface of the layers to improve the compatibility with hydrophobic nonpolar monomers/polymers; (2) increase interlayer distance; and (3) form "porous pathways" via the random arrangement of methyl and hydroxyl groups in the interlayer space, since the two groups have different dimensions.[47] Such an arrangement can break the ordered structure and create an irregular, porous interlayer structure, which will help expedite the intercalation/exfoliation rate.[47] A higher concentration of methyl groups in the interlayer space is expected to be beneficial for improving compatibility. However, too high a concentration of methyl groups is disadvantageous to the formation of "porous pathways", and it might also negatively affect the synthesis of the derivative. Out of the above considerations, three ZrP(Me/OH) mixed derivatives were designed by adjusting the formulation ratio of methylphosphonic acid and phosphoric acid, as shown in Table 1.

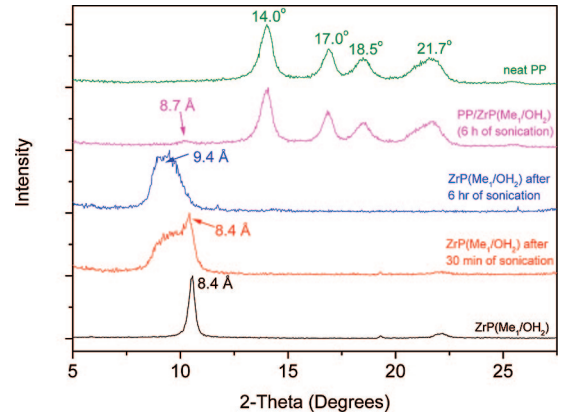

Figure 4. XRD pattern of $ZrP(Me_1/OH_2)$ and $PP/ZrP(Me_1/OH_2)$ nanocomposite.

The XRD patterns of the synthesized α-ZrP and ZrP(Me/OH) mixed derivatives are presented in Figure 2. As designed and expected, ZrP(Me/OH) mixed derivatives have a larger interlayer distance than the 7.6 Å interlayer distance of α-ZrP.[57] This is because a methyl group has a larger dimension than a hydroxyl group the interlayer-spacing of $Zr(O_3PCH_3)_2$ being 8.9 Å. As higher concentrations of methylphosphonic acid were used in the formulation, the correspondingly prepared ZrP(Me/OH) mixed derivative exhibited increased interlayer distances from 8.4 to 8.8 Å. The question of the distribution of mixed ligand compounds of zirconium has been treated by Rosenthal and Caruso.[58] If the distribution is random but there is an excess of the smaller-sized ligand, the interlayer spacing should be half the sum of the two independent layer sizes, in this case, 8.25

(57) Troup, J. M.; Clearfield, A. *Inorg. Chem.* **1977**, *16*, 3311–3314.
(58) Rosenthal, G. L.; Caruso, J. *J. Solid State Chem.* **1993**, *107*, 497–502.

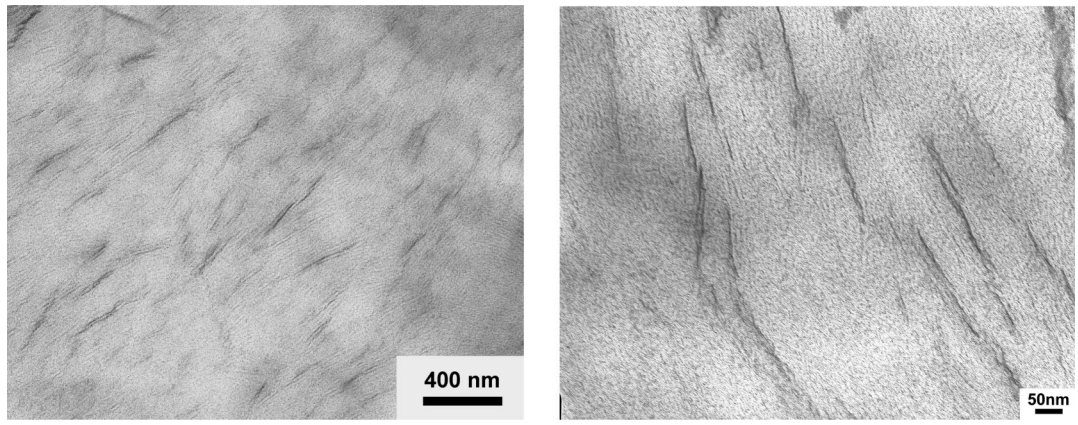

Figure 5. TEM images of PP/ZrP(Me_1/OH_2) nanocomposite prepared with ultrasonicated ZrP(Me_1/OH_2).

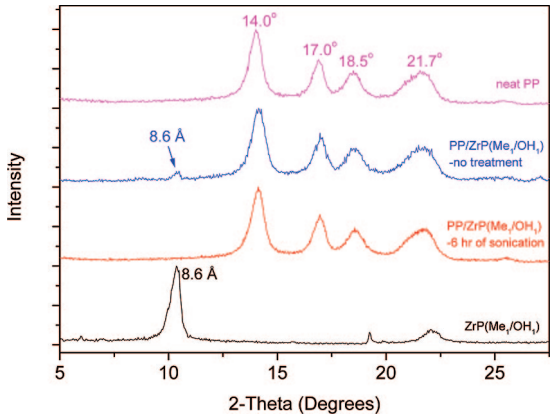

Figure 6. XRD pattern of PP/ZrP(Me_1/OH_1) nanocomposites.

Å. However, it is seen in Figure 2 that there is a progressive increase in the interlayer spacing. Even when the methyl groups are in the minority, the spacing is still greater than 8.25 Å. Either more methyl groups were taken up than phosphoric acid groups or some of the methyl groups rest in between methyl groups adjacent to P-OH groups on opposite layers, resulting in a gradual approach to the upper limit of 8.9 Å.

A larger interlayer distance is beneficial for the subsequent intercalation/exfoliation process. However, an even larger benefit might be attributed to the formation of "porous pathways" within the gallery space.[47] Such a "porous pathway" structure has been proved to be advantageous to the intercalation of monomers, compared with highly ordered packed interlayer space, which may have an even larger interlayer distance.[47] The relatively larger peak width of the XRD patterns of ZrP(Me/OH) mixed derivatives also indicates that the layered structure of these derivatives is not as uniform as that of α-ZrP, which also suggests the formation of irregular "porous pathways".

The SEM images of α-ZrP and the three ZrP(Me/OH) mixed derivatives are presented in Figure 3. It shows that similar to α-ZrP, ZrP(Me_1/OH_2) and ZrP(Me_1/OH_1) still exhibit a sheet structure, with a lateral dimension of approximately 1 μm, which is close to the size of α-ZrP. This supports the notion that the introduction of relatively low concentrations of methyl groups into the layered structure does not lead to significant changes in crystal shape and dimension. Unlike the above two mixed derivatives, ZrP(Me_2/OH_1) does not form sheet structured crystals. Its semicrystalline morphology shown in Figure 3D is consistent with its low crystallinity as evidenced by the low intensity X-ray diffraction peaks shown in Figure 2. Thus, only two of the derivatives, ZrP(Me_1/OH_2) and ZrP(Me_1/OH_1), were chosen for the preparation of PP nanocomposites. The above results also suggest that a certain concentration of phosphoric acid is necessary to form good crystal structures when synthesizing α-ZrP mixed derivatives.

Preparation of PP/ZrP(Me/OH) Nanocomposites. It is expected that the incorporation of methyl groups onto the layer surface would improve the compatibility of ZrP(Me/OH) mixed derivatives with toluene and propylene molecules. However, the initial attempt to disperse ZrP(Me_1/OH_2) in toluene without any treatment was not successful. The ZrP(Me_1/OH_2) derivative failed to form a stable dispersion. After standing still for a short period of time, the ZrP(Me_1/OH_2) derivative precipitated. Thus, nontreated ZrP(Me_1/OH_2) was not chosen for the preparation of PP nanocomposites.

To promote the dispersion of ZrP(Me_1/OH_2) in toluene, an ultrasonication treatment was adopted. An initial 30 min ultrasonication treatment effectively dispersed part of the ZrP(Me_1/OH_2), leading to the formation of ZrP(Me_1/OH_2) gels. A portion of the ZrP(Me_1/OH_2) appeared to remain intact and precipitated after being left to stand. The XRD pattern of a dried ZrP(Me_1/OH_2) sample after 30 min of ultrasonication is presented in Figure 4. The pattern shows that the diffraction peak corresponding to the interlayer structure has been significantly broadened, but the original peak still exists. This suggests that 30 min of ultrasonication has only dispersed part of ZrP(Me_1/OH_2). Therefore, the ultrasonication treatment was extended to 6 h, which helped fully disperse ZrP(Me_1/OH_2) in toluene. As the XRD pattern of a dried sample (Figure 4) shows, the original peak at 8.4 Å was completely removed after 6 h of ultrasonication treatment and the diffraction peak has been significantly broadened. The average interlayer distance was increased to approximately 9.4 Å. The increase of interlayer space and the broadened peak indicate that ZrP(Me_1/OH_2) has been intercalated by toluene molecules with the help of ultrasonication. In contrast, a control experiment indicates that 6 h

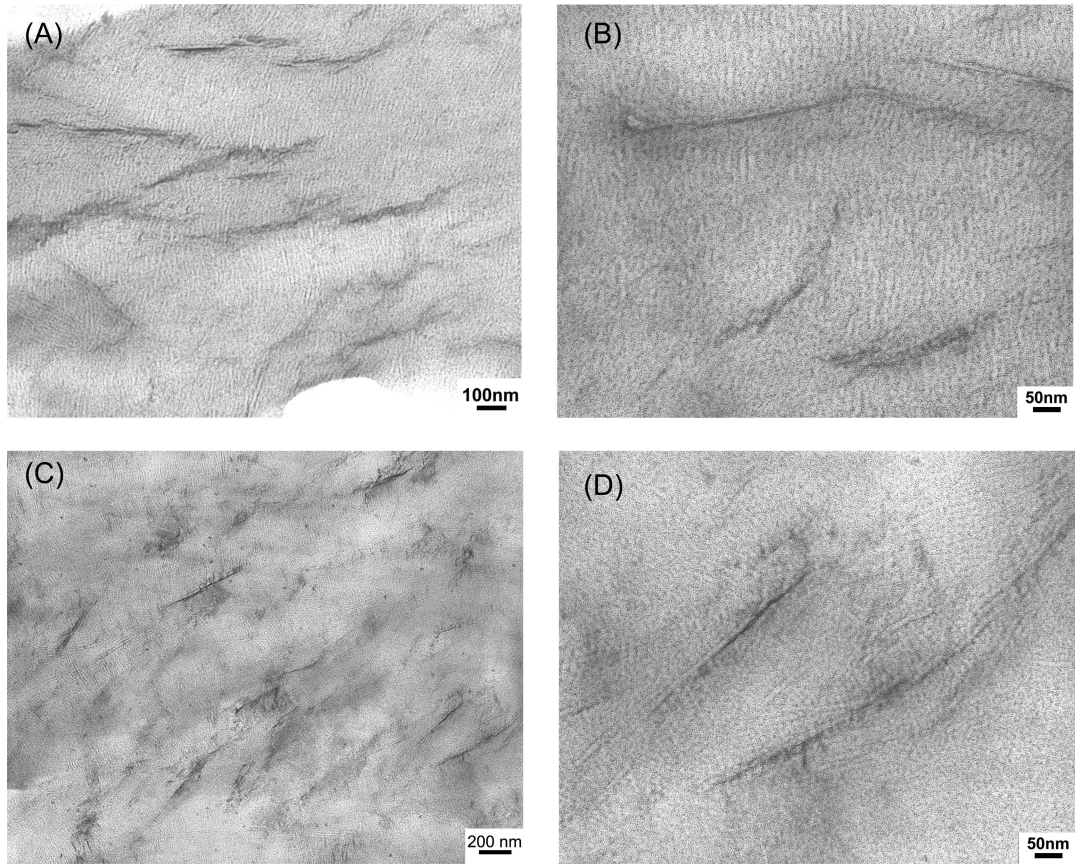

Figure 7. TEM images of PP/ZrP(Me_1/OH_1) nanocomposites: (A, B) sample prepared with ultrasonicated ZrP(Me_1/OH_1); (C, D) sample prepared with pristine ZrP(Me_1/OH_1).

of ultrasonication treatment at the same condition does not lead to any interlayer distance change in pristine α-ZrP.

The toluene solvated ZrP(Me_1/OH_2) was subsequently used to prepare isotactic PP nanocomposites. As anticipated, the activity of the catalyst system decreased upon addition of ZrP(Me/OH), in spite of the increased level of activator used. A slight decrease in isotacticity was observed, but this was determined to be acceptable. The XRD pattern of a PP/ZrP(Me_1/OH_2) nanocomposite was also recorded (Figure 4). A tiny hump at around 8.7 Å was observed, which indicated that a small amount of ZrP(Me_1/OH_2) remained intercalated, whereas most of ZrP(Me_1/OH_2) has been exfoliated after in situ polymerization.[59] To be noted, the tiny hump is located at the higher angle shoulder of the interlayer structure peak (9.4 Å) of toluene solvated ZrP(Me_1/OH_2). This indicated that the layers with relatively larger interlayer space have been exfoliated. The remainder is mainly material not well intercalated during the ultrasonication treatment. With a higher power and/or more effective ultrasonication treatment, an even better exfoliation result is expected.

The TEM images of PP/ZrP(Me_1/OH_2) nanocomposite prepared from ultrasonicated ZrP(Me_1/OH_2) are shown in Figure 5. The images show that ZrP(Me_1/OH_2) nanoplatelets have been uniformly dispersed in the PP matrix. However, full exfoliation was not achieved. Some of the nanoplatelets have a thickness of 5−10 nm. This suggests that those nanoplatelets still consist of multilayers, which is consistent with the XRD results shown in Figure 4.

The unsuccessful dispersion of ZrP(Me_1/OH_2) in toluene without ultrasonication and the unsuccessful attempt to completely exfoliate ultrasonicated ZrP(Me_1/OH_2) during the in situ polymerization is possibly due to the insufficient compatibility between ZrP(Me_1/OH_2) and hydrophobic molecules (e.g., toluene, propylene). To further improve their compatibility, ZrP(Me_1/OH_1) was synthesized as described above.

ZrP(Me_1/OH_1) was also ultrasonicated and then subjected to in situ polymerization via the same procedures described above. The XRD pattern of the prepared PP/ZrP(Me_1/OH_1) nanocomposite is shown in Figure 6. No diffraction peaks corresponding to intercalated ZrP(Me_1/OH_1) or pristine ZrP(Me_1/OH_1) were observed, which shows an improvement compared to PP/ZrP(Me_1/OH_2) prepared via the same approach. The TEM images of the nanocomposite sample are

(59) A large body of literature has been dedicated to the study of single-site polymerization catalysts immobilized on heterogeneous supports (see, for example, Hlatky, G. G. *Chem. Rev.* **2000**, *100*, 1347–1376). Marks and others have carefully examined the interaction of zirconocenes with silica, alumina, and other oxide supports. See, for example, (a) Hicks, J. C.; Mullis, B. A.; Jones, C. W. *J. Am. Chem. Soc.* **2007**, *129*, 8426–8427. (b) Marks, T. J. *Acc. Chem. Res.* **1992**, *25*, 57–65. (c) Motta, A.; Fragalà, I. L.; Marks, T. J. *J. Am. Chem. Soc.* **2008**, *130*, 16533–16546. (d) Nicholas, C. P.; Ahn, H.; Marks, T. J. *J. Am. Chem. Soc.* **2003**, *125*, 4325–4331. (e) Nicholas, C. P.; Marks, T. J. *Langmuir* **2004**, *20*, 9456–9462, It is conceivable, in light of this work, that MAO (or residual free trimethylaluminium contained therein) could react with a surface hydroxyl group of α-ZrP, yielding a reactive site. A molecule of the zirconocene catalyst precursor could then attach to this site, forming an immobilized catalytic site. A polymer chain growing from this site would serve to push the layers of the α-ZrP apart, enhancing exfoliation.

displayed in images A and B in Figure 7. The images show that ZrP(Me_1/OH_1) nanoplatelets are well-dispersed and highly exfoliated in the PP matrix, although some of the exfoliated ZrP(Me_1/OH_1) nanoplatelets may still contain a few stacked layers based on the nanoplatelet thickness from TEM image as shown in Figure 7B.

Unlike ZrP(Me_1/OH_2), which failed to form a stable toluene dispersion without any ultrasonication treatment, ZrP(Me_1/OH_1) can be well-dispersed in toluene to form a gel-like dispersion once it is mixed with toluene after brief mechanical shaking. The quick dispersion of ZrP(Me_1/OH_1) in toluene can be attributed to the formation of a "porous" interlayer structure, which expedites the migration of toluene into the nanoplatelet gallery. The gel-like dispersion remained stable after 24 h of storage. The increased dispersibility of ZrP(Me_1/OH_1) in toluene can be attributed to its higher hydrophobicity, larger interlayer space, and better formed "porous pathway" structure.[47] The ZrP(Me_1/OH_2) toluene dispersion was thus directly used for the preparation of PP nanocomposites.

The XRD pattern of the PP/ZrP(Me_1/OH_1) nanocomposite prepared using nontreated ZrP(Me_1/OH_1) is presented in Figure 6. A tiny hump corresponding to an interlayer distance of 8.6 Å is visible on the XRD pattern, which indicates that part of ZrP(Me_1/OH_1) sample remained intact after it was dispersed in toluene and subjected to subsequent in situ polymerization. The TEM images of PP/ZrP(Me_1/OH_1) nanocomposite in images C and D in Figure 7 confirm that a high level of exfoliation has been achieved, which is close to the one prepared from the ultrasonicated ZrP(Me_1/OH_1). The thickness of the nanoplatelets in the TEM images suggests the existence of multiple stacked layers, which is consistent with its XRD pattern.

By introducing more methyl groups onto the interlayer surface, the ZrP(Me_1/OH_1) mixed derivative exhibits higher compatibility with organic solvent and the PP matrix than ZrP(Me_1/OH_2). This trend indicates that the introduction of methyl groups onto α-ZrP does effectively improve the hydrophobicity of the α-ZrP derivative as expected. The synthesized α-ZrP derivatives function as the organically treated clay, but with a much better thermal and chemical stability, because the grafted organic functional groups are covalently bonded to the layers, rather than weakly interacted by electrostatic force in ion exchanged clays. Unfortunately, further increasing methyl group concentration in the formulation did not lead to sheet structured nanoplatelets, which inhibits further exploration in this direction. Attempts to prepare other ZrP(alkyl/OH) mixed derivatives with larger interlayer distance for polymer nanocomposite applications are underway. To be noted, besides alkyl groups, other groups, such as phenyl, can also be incorporated onto the interlayer surface by using the corresponding phosphonic acids. Such α-ZrP derivatives should find applications in nanocomposites and other fields, such as fuel cell membranes.

Conclusions

The present study has demonstrated that the surface hydrophobicity of ZrP(Me/OH) mixed derivatives can be tuned by adjusting the synthetic formulation. The ZrP(Me/OH) mixed derivatives with higher hydrophobicity and larger interlayer space exhibit much higher compatibility with toluene and propylene. Isotactic PP-based nanocomposites have been successfully prepared by using the designed ZrP(Me/OH) mixed derivatives with brief or no pretreatments. The PP nanocomposites show a high level of exfoliation. Direct synthesis of α-ZrP based nanoplatelets with designed surface functionality has been shown to be a promising and effective approach for the preparation of PP nanocomposites.

Acknowledgment. This work was sponsored by Specialty Minerals Inc., for which grateful acknowledgment is made. The authors also gratefully acknowledge the partial financial support of the National Science Foundation (DMR-0652166), the Defense Logistic Agency (SP0103-02-D-0024), and the State of Texas ATP Grant (000512-00311-2003). The SEM acquisition was supported by the National Science Foundation under Grant DBI-0116835. L.S. thanks Dr. Deyuan Kong for valuable discussions.

Supporting Information Available: Additional tables, synthesis information, and structural drawing (PDF); crystallographic information in CIF format. This material is available free of charge via the Internet at http://pubs.acs.org.

CM803024E